THESIS FOR THE DEGREE OF LICENTIATE

Frequency combs on chip for interferometry applications

Israel Rebolledo Salgado

CHALMERS

Photonics Laboratory
Department of Microtechnology and Nanoscience (MC2)
Chalmers University of Technology
Göteborg, Sweden, 2022

Frequency combs on chip for interferometry applications
Israel Rebolledo Salgado

ISSN 1652-0769
Technical Report MC2-452

Photonics Laboratory
Department of Microtechnology and Nanoscience (MC2)
Chalmers University of Technology
SE–412 96 Göteborg
Sweden
Telephone: +46 (0)31–772 10 00

Printed in Sweden by
Reproservice
Chalmers Tekniska Högskola
Göteborg, Sweden, 2022

Frequency combs on chip for interferometry applications

Israel Rebolledo-Salgado
Photonics Laboratory
Department of Microtechnology and Nanoscience (MC2)
Chalmers University of Technology

Abstract

Optical frequency combs have revolutionized the field of laser spectroscopy. A frequency comb is a type of laser that generates an array of equally spaced coherent laser lines. Indeed, the outstanding performance of frequency combs in terms of bandwidth and stability is readily attainable in bench-top systems. Integrated photonics offers a platform for the implementation of frequency combs relying on nonlinear optics processes.

This thesis explores the generation of chip-scale frequency combs based on supercontinuum and microcomb generation and its potential use for interferometry. This investigation covers the capabilities offered by supercontinuum generation in the normal dispersion regime. The spectral broadening is realized by pumping a straight waveguide with a short duration pulse meaning that the pump is a comb itself. Therefore, its performance in terms of coherence and the transferring of noise to the broadened spectra have been investigated. Microcombs can be generated on a microresonator starting from a continuous wave laser. In this work, we study microcomb generation in the normal dispersion regime using a novel dual-cavity architecture.

The appended papers describe the nonlinear processes involved in the microcomb generation. We have studied its capabilities in terms of spectral flatness and symmetry, together with the coherence attained on these combs. It is found that these capabilities make microcombs a suitable spectral sources for spectroscopy. Furthermore, the capabilities of different interferometry techniques are analyzed in terms of resolution, sensitivity and measurement time in order to perform on-chip dual-comb spectroscopy.

Keywords: optical frequency combs, microcombs, pulses, nonlinear optics, interferometry, integrated photonics, spectroscopy

Publications

This thesis is based on the work contained in the following papers:

[A] Israel Rebolledo-Salgado, Zhichao Ye, Simon Christensen, Fuchuan Lei, Krishna Twayana, Jochen Schröder, Martin Zelan, and Victor Torres-Company, "Coherent supercontinuum generation in all-normal dispersion Si_3N4 waveguides", *Optics Express*, 30, 8641-8651, 2022.

[B] Israel Rebolledo-Salgado1, Óskar B. Helgason, Zhichao Ye, Jochen Schröder, Martin Zelan, and Victor Torres-Company, "Photonic molecule microcombs at 50 GHz repetition rate", *Conference on Lasers and Electro-Optics*, San Jose, USA, paper SW4O.8, 2022.

[C] Krishna Twayana, Israel Rebolledo-Salgado, Ekaterina Deriushkina, Jochen Schröder, Magnus Karlsson and Victor Torres-Company, "Frequency-comb-based spectral interferometry for characterization of photonic devices", *Micromachines*, 13, no 4, p. 614, 2022.

Related publications and conference contributions by the author, not included in the thesis):

[D] I. Rebolledo-Salgado, Z. Ye, S. Christensen, F. Lei, J. Schröder, M.Zelan, V. Torres-Company "Nonlinear Broadening of Electro-Optic Frequency Combs in All-Normal Dispersion Si_3N_4 Waveguides", *Proceedings of Conference on Lasers and Electro-Optics Europe/ European Quantum Electronics Conference (CLEO/Europe-EQEC)*,2021, pp. 1-4

[E] E. Deriushkina, I. Rebolledo-Salgado, M. Mazur, V. Torres-Company, P. Andrekson, S. Gross, M.J Withford, T. Hayash, T. Nagashima, J. Schröder, M. Karlsson "Characterisation of a

Coupled-Core Fiber Using Dual-Comb Swept-Wavelength Interferometry" *Proceedings of European Conference on Optical Communication (ECOC)*,2021, pp. 1-1

Contents

Acknowledgements

First and foremost, I would like to thank my supervisor, Professor Victor Torres-Company, my sincere gratitude for all the support, and encouragement and for always inspiring me to go further. A big thanks to my co-supervisor Martin Zelan, for all the scientific insights and immense encouragement he has provided me. I am also grateful to Dr. Jochen Schröder, Prof. Peter Andrekson, and Prof. Magnus Karlsson for sharing knowledge and insights.

I am thankful to work closely with the bright and wonderful people members of the Ultrafast Photonics group. Dr. Zhichao Ye deserves a big acknowledgment because his excellent fabrication made possible much of this work. I also would like to thank Dr. Francisco Artega and Dr. Simon Christensen for all the help and insights on the supercontinuum generation. Dr. Oskar Helgasson also deserves my gratitude for all the help in the lab and for teaching me about microcombs. I am also thankful to Dr. Fuchual Lei for sharing all his knowledge and curiosity. I appreciate having Krishna Twayana as my office mate for all the help and long conversations about science and football. Special thanks to Marcello Girardi for being an amazing colleague and friend, and for always sharing his knowledge about photonics and python programming.

I am thankful to all the current and former members of the Photonics lab for creating such a nice environment of working. Special thanks to Dr. Kovendhan Vijayan, Ali Mirani for sharing their knowledge about fiber optics and always being willing to help. I also thank Ekaterina Deriushkina for the experiments we performed together and the nice discussions about interferometry.

Life in Göteborg has been easier having many amazing friends surrounding me, but I want to express special thanks to Annaleena, Gaby, and Felix for the nice moments shared. Finally, I would like to express my gratitude to the most important person in my life, my beloved Wendy, for all the support, patience, and love.

Chapter 1

Introduction

The spectral nature of light can be readily seen on a rainbow after rain showers. Although this phenomenon marveled people for thousands of years, the presence of colors was merely a curiosity without any scientific significance. This changed in the 17th century when Isaac Newton realized the separation of sunlight into a series of colors, introducing the concept of a spectrum for first time. In his experiments, he used an arrangement composed of a lens, a prism and screen to analyze the light. The invention of this first spectrograph, and the later work on the observation of dark lines in the solar spectrum made by Wolleston and Fraunhofer, established the beginning of modern spectroscopy [1].

Optical spectroscopy is nowadays an ubiquitous tool in research and industry since it offers the characterization of samples with high sensitivity and non-destructive testing. Optical spectrometers have been applied to an extensive number of applications including biochemical environmental sensing [2], gas absorption spectroscopy [3, 4] and the characterization of telecommunication components. Ultra-high resolution measurements are attainable with modern spectrometers, for example, based on dispersive elements. In traditional grating-based designs, the light is spatially separated and projected onto a photo-detector array.

Another approach is using Fourier-transform (FT) spectrometers based on scanning interferometric systems. Indeed, Fourier-transform spectrometry based on a Michelson interferometer is a well-established tool for molecular spectroscopy using thermal sources [5]. Using such configuration, an optical signal is split in two optical paths, one with a different length which will cause a temporal delay. The two arms are then combined and an interference pattern is obtained from the super-

position of the original optical signal with its delayed copy. This type of spectrometers can record well-resolved spectra, however it requires long scanning ranges.

The use of this conventional setups can deliver outstanding performance but they rely on large instrumental setups due to the inherent relation between resolution and optical path length. It is often that applications such as industrial monitoring processes, medical diagnosis [6,7] or food quality monitoring [8] do not require ultra-high resolution but instead need compact systems that can perform on-spot measurements. Thus, a trend towards the miniaturization of spectrometers has emerged during the last years. The miniaturization of spectrometers can enable portability, the reduction of footprint, power consumption and a massive fabrication [9]. There is also an increased interest on embedded microspectrometers on smartphones for bio-sensing taking advantage of the data processing power of mobile computing [6, 10].

However, the reduction of spectrometers poses a challenge due to the competing requirements in terms of size and performance. Many approaches have looked into the possibility of mimic the bench-top strategy based on dispersive and interferometric techniques [11–13]. Several demonstrations of on-chip spectrometers have been reported using photonic integrated circuits such as waveguides and gratings to perform a similar task as free-space optics components [14–16]. The recent work has mainly focused on a dispersive configuration, for example using arrayed waveguide gratings, however, a trade-off between the footprint size and resolution still remains [17–19]. Furthermore, such configuration suffers from high signal to noise ratio penalties due to the spreading of light into different channels. This is not the case for FT spectrometers, which benefits of a multiplexing advantage where many spectral components are measured simultaneously. Different approaches have been explored towards the integration of FT spectrometers [13, 20, 21]. In traditional FT spectrometers, the movement of mirrors is performed to tune the optical path length. In photonic planar technologies this is achieved using a thermo-optic modulation effect or employing arrays of discrete integrated interferometers, i.e. a large number of channels is employed [22, 23]. Although boosted SNR and high resolution are possible, reducing the chip footprint is an on-going topic of investigation towards the scalability of dispersive and FT spectrometers.

Notwithstanding, the aforementioned techniques, either in a bench-top or compact configuration, have proved to be robust and fruitful. It

was not until the introduction of the laser that spectral resolution and sensitivity were increased by several orders of magnitude [24]. For example, in order to record well-resolved spectra, FT spectrometers require long scanning ranges which is challenging due to the low spatial coherence of the light sources employed [25]. The advent of the laser led to a revolution in optical interferometry since it provided an intense source of light with a high degree of temporal and spatial coherence. This, in turn, translates into highly sensitive measurements with high spectral resolution limited only by the linewidth of the laser.

These qualities stimulated numerous applications of laser spectroscopy and consequently the technical development of new laser sources. A significant aspect in the application of lasers for spectroscopy is the emission region. Arguably, the most appealing is the mid-IR and far-IR since many chemical substances have vibrational transitions that can be probed directly. Laser spectroscopy is of significant relevance for monitoring the concentration of greenhouse gases, in medical diagnosis and chemical analysis just for mention a few. A significant limitation is the reduced spectral bandwidth offered by tunable lasers used in this applications.

In recent years, a new type of laser called frequency comb has revolutionized optical spectroscopy [26, 27]. The unique feature of frequency combs is that it possesses broad spectral emission composed of discrete evenly spaced laser lines. Thus, spectroscopy using frequency combs combines a large spectral span (a distinctive characteristic of FT spectroscopy using incoherent sources) with the narrow linewidth resolution and high intensity offered tunable laser spectroscopy.

Frequency combs have undoubtedly followed the general path towards integrated systems [28]. Since the early demonstrations using microcavities in 2007 [29], the research field has exploded during the last years. Microresonator-based frequency combs, or microcombs, are generated from a single frequency continuous wave laser through optical nonlinearities.

The first demonstrations of microcombs were based on whispering gallery mode resonators and have spread over a large number of fabrication technologies and materials [28].

Microcomb generation relies on the interplay of nonlinear processes and dispersion on a microcavity. Indeed, the generation of microcombs has been explored in different material platforms that offer high nonlinearities and the possibility of dispersion engineering. Silicon nitride

stood out for its compatibility with CMOS processes and a large transparency window which makes it suitable for different applications [30]. Silicon nitride also enables high optical confinement which is key for nonlinear mechanisms due to the large refractive index contrast with silica cladding materials.

Frequency combs on a chip-scale offer the possibility of taking the frequency comb capabilities out of research laboratories. Such combs usually show high repetition rates and broad spectral bandwidth, which applied to spectroscopy, enable parallel detection of multiple species at the expense of large the spectral sampling. Recent works have also demonstrated the use of on-chip frequency combs as a light source for LIDAR and optical coherence tomography systems [31, 32]. Another implementation, based on the established dual-comb technique employs on-chip dual comb sources for spectroscopy exploiting its high degree of relative coherence have been also demonstrated [33–35].

1.1 This thesis

This thesis focuses on the study of the generation of chip-scale frequency combs to extend its capabilities to broadband optical spectroscopy. The chip-based frequency combs are realized through supercontinuum generation (SCG) in optical waveguides and Kerr-comb generation in microresonators. It is found that these frequency comb sources can provide stable and coherent spectra over a broad spectral range. Furthermore, the capabilities of different interferometry techniques based on established frequency combs sources are analyzed in order to perform on-chip spectroscopy, specifically in a dual-comb configuration.

The supercontinuum generation is implemented in the silicon nitride platform which is appealing due to the high nonlinear coefficient and the absence of nonlinear absorption losses. Furthermore, there is an interest in operating in the normal dispersion regime since it allows the coherent broadening of spectra using long duration pulses. Therefore, a thorough investigation of the coherence properties has been performed [Paper A].

An important challenge in the frequency comb generation using microresonators is the usable power per comb line achieved. Microcombs generated in cavities that exhibit normal dispersion have shown to offer a high conversion efficiency, which means that high signal-to-noise ratio can be achieved. The generation of microcombs in the normal dispersion regime is also appealing since it relaxes the dispersion engineering

requirements. This is due to the fact that bulk materials such as silicon nitride exhibits strong normal dispersion, working in this regime also enables the possibility of comb generation in a large spectral window.

Another practical aspect is the initiation of microcombs, by using a dual-cavity architecture it is possible the deterministic operation of microcombs. This architecture, also referred as photonic molecule has been explored in paper B for the generation of microcombs in the normal dispersion regime using a mode-coupling interaction for the initiation. As a consequence, a symmetric spectral envelope is obtained and the resilience of the repetition rate of the microcomb is observed. The integration of this technology offers the possibility of realizing chip-scale spectrometers that cover broad spectral bandwidths with a resolution given by the comb line teeth. The application of frequency combs for linear spectroscopy techniques is also provided as part of this study [paper C].

Chapter 2

Optical frequency combs

The main focus of this thesis is the application of optical frequency combs on interferometry. In this chapter a general description of frequency combs is provided along with the different mechanisms to generate them. Furthermore, some examples of comb-based spectroscopy is given.

2.1 General description of frequency combs

In optical spectroscopy there is a need to measure the frequency of the light rather than its wavelength in order to have more accurate results. Measuring frequency means counting the number of cycles over certain period of time and the accuracy of the measurement is in principle limited only by reference clock used. The measurement of high frequencies is restricted due to the limitations in the available electronics to the radio-frequency (RF) domain (up to 100 GHz). This range is well below the optical frequencies (>100 THz). A way to circumvent this, is by the use of harmonic frequency chains, which have enabled measurements of visible light. Such chains were based on a stable 100 MHz reference that was multiplied over a large factor to reach optical frequencies. However, this method required a large complex setup with the size of a full facility and it can only measure a single optical frequency [36]. The generation and control of a mode-locked laser replaced this technique and enabled the measurement of absolute optical frequencies [37, 38]. This type of laser, referred to as an optical frequency comb, provided a bi-directional connection between the radio-frequency and optical domains [39].

In the frequency domain, an optical frequency comb can be defined as a laser source that emits a series of narrow frequency lines that are

equally spaced. In the time domain, the output of the frequency comb laser consists of a pulse train with a constant repetition rate (f_{rep}), which is the inverse of the frequency separation. Likewise, the frequency comb can be assumed as a source of pulses with a carrier frequency (f_c) that is modulated by a pulse envelope $A(t)$. It can be represented as a Fourier series, therefore, the electrical field of the comb can be represented as:

$$E(t) = Re(A(t)\exp(i2\pi f_c t)) = Re(\Sigma_n A_n \exp(i(f_c + nf_{rep})t)), \quad (2.1)$$

where A_n are the Fourier components of $A(t)$ and f_{rep} is the repetition frequency of the comb. Given f_c is not an exact multiple of the repetition rate, the spectral lines of the comb are all shifted by a common offset frequency f_0. The frequency comb can be fully described if the carrier envelope offset frequency (f_0) and the repetition rate are known. Hence, the absolute optical frequency of each comb line (f_n) is represented by:

$$f_n = f_0 + nf_{rep}. \quad (2.2)$$

This equation manifests that the comb can be described in terms of two frequencies, usually in the radio-frequency domain. It also shows that optical frequencies are straightforwardly reached by multiplying a microwave frequency f_{rep} by a factor n, which is usually in the order of $10^5 - 10^6$. Equation 2.2 is commonly referred to as the comb equation, showing that with the information of these two frequencies, any optical frequency of the comb can be labeled with the precision and accuracy of f_0 and f_{rep}.

2.1.1 Mode-locked lasers

The foundations of frequency combs can be traced back to 1960, with the experimental demonstration of an active mode-locked laser (MLL) using a Q-switching method [40]. This technique utilized an active modulation of the internal losses of the cavity to control the Q-factor of the resonator. A passive scheme of mode-locking was proposed by replacing the modulators with a fast saturable absorber [41]. The sketch of a MLL setup using a passive scheme is depicted in Figure 2.1 (a).

Later work used the Kerr-lens effect to achieve mode-locking using a Ti:sapphire crystal as the gain medium [42]. Ti:sapphire lasers became

the most widespread configuration since they provide wide spectral bandwidths and generation of femtosecond pulses. However, these techniques did not include an active feedback stabilization and as a consequence, a dephasing of the pulses occurred due to perturbations in the cavity.

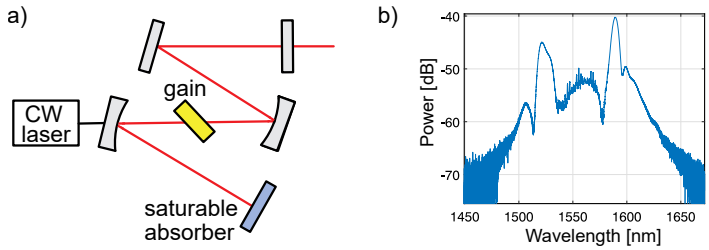

Figure 2.1: Mode-locked laser. (a) Basic setup of a mode-locked laser, where a gain medium is placed in the cavity and a saturable absorber mirror is used to achieve passive mode locking. (b) The measured spectrum of a femtosecond mode-locked laser from Menlo systems, the spectral envelope is not resolved by the optical spectrum analyzer and appears to be continuous due to the low repetition rate of 100 MHz.

Mode-locked lasers have been used for frequency comb generation since their early days, in fact, many commercial systems still use them (see Figure 2.1 (b)). In the following, an MLL laser will be used as an example to provide a better grasp of the frequency comb structure.

The repetition rate (f_{rep}). In the time domain, the output of a MLL is a series of consecutive pulses with a time separation T_r related to the length of the laser cavity that can be expressed as follows:

$$T_r = \frac{1}{f_{rep}} = \frac{L}{\nu_g}, \tag{2.3}$$

where f_{rep} is the repetition rate of the frequency comb, L is the length of the cavity, and ν_g is the group velocity of the pulse. This relation indicates that variations in the cavity length can contract or expand the repetition rate in an accordion-like fashion. Meaning that the repetition rate determines the pulse to pulse time and the separation of the frequency lines of the comb.

The pulses of the mode-locked laser are conformed by massive amplitude modulation of all different optical modes of the comb. These pulses measured by heterodyne detection will produce a number N of

frequency harmonics of the repetition rate. However, it does not provide information on the offset frequency since it is a common frequency for the comb. If a direct optical detection of two frequency modes (m and n) is considered, the beat note measured will yield information on the repetition rate only, i.e.,

$$\nu_m - \nu_n = (f_0 + m f_{rep}) - (f_0 + n f_{rep}) = (m - n) f_{rep}. \tag{2.4}$$

Therefore, the control of the repetition rate frequency can be easily performed since it can be measured using a sufficiently fast photodetector.

The frequency offset (f_0). As mentioned before, a key feature of a frequency comb is the ability to measure and control its repetition rate (f_{rep}) and the offset frequency (f_0). The detection of f_0 is more difficult since it is related to the phase of the consecutive pulses. In a MLL, this arises due to the fact that the pulses coming out are not fully identical due to dispersion in the cavity. Instead, a phase shift $\Delta\phi = 2\pi f_0 / f_{rep}$ between the peak of the envelope and the nearest peak of the carrier wave occurs as shown in Figure 2.2 (a). This phase variation $\Delta\phi$ evolves from pulse to pulse and translates in a frequency shift f_0 of the complete comb (Fig. 2.2 b).

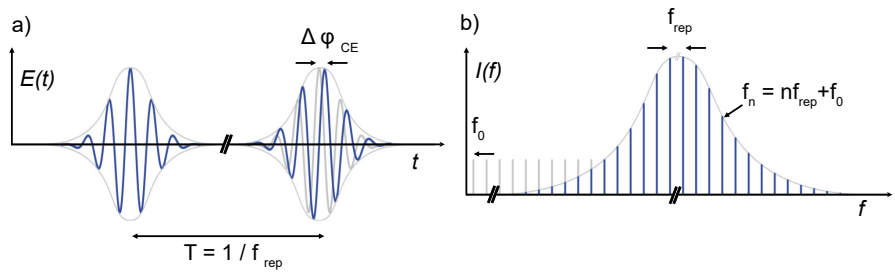

Figure 2.2: (a) Time-domain representation of an optical frequency comb. (b) In frequency domain the OFC consist of a broad spectrum of equally spaced comb lines, whose optical frequencies are given by $f_n = n f_{rep} + f_0$.

In order to assess f_0 directly, one would need to measure the oscillations of the carrier, which is impossible with the current electronics bandwidth.

2.1.2 Self-referencing

A method to determine the offset frequency was proposed in [43,44] using a nonlinear conversion method. This technique, called self-referencing, uses a $f-2f$ interferometer and requires that the bandwidth of the frequency comb spans more than one octave. For this reason, the spectral broadening of femtosecond mode-locked lasers using highly nonlinear fiber was a key development in the frequency comb stabilization [38, 44, 45]. An sketch of the self-referencing method using a broadened frequency comb that spans an optical octave is shown in figure 2.3. In a $f-2f$ interferometer, a comb mode in the low-frequency side is doubled using a nonlinear crystal and interfered with a comb mode that is twice the frequency, providing the offset frequency beat note as:

$$2(nf_{rep}+f_0)-(2nf_{rep}+f_0)=f_0. \tag{2.5}$$

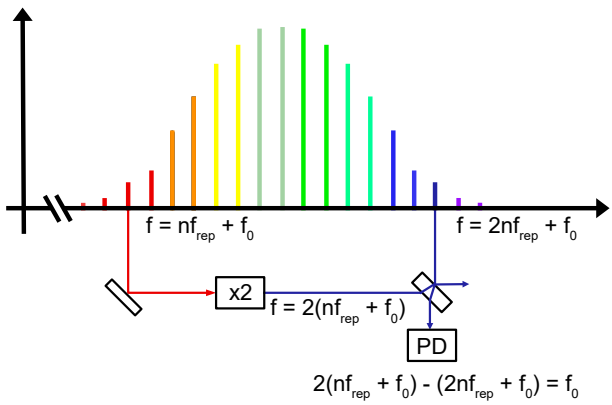

Figure 2.3: Self-referencing technique using a $f-2f$ method. A mode n at the red side of the spectrum is frequency doubled using a nonlinear crystal. If the frequency comb covers a full optical octave span, a mode $2n$ with a frequency $2nf_{rep}+f_0$ is located in the blue side- The beat note between the doubled-frequency mode and the $2n$ yields the offset frequency.

Although full stability of MLL is achieved and has been extensively exploited, their frequency spacing and central frequency are mainly fixed and determined by the specific design. Furthermore, some applications such as communications, imaging, and RF photonics do not require self-referencing but they demand higher flexibility in repetition rate (frequency spacing) [46].

2.2 Electro-optic frequency combs

Electro optic (EO) combs are based on electro-optic modulation. In short, a CW laser is modulated by a microwave signal such that sidebands to the laser spectrum are generated, where the central and repetition frequencies are defined by the frequency of the laser and the modulation frequency respectively. These two parameters can be chosen freely within the operation bandwidth of the modulators, providing a simple yet powerful technique to generate a comb. Together with these degrees of freedom, the EO comb generators can be directly shaped to synthesize different temporal waveforms [46, 47].

2.2.1 Generation

Several configurations of electro-optic combs have been implemented with the purpose of obtaining flat spectral envelopes, which are appealing for spectroscopy and communication applications. In this section, a configuration using cascaded phase and intensity modulators will be discussed since this approach has been employed for the work presented in paper A.

The modulators work under the Pockels electro-optic effect where the refractive index varies in the presence of an electric field. We can start considering a single phase modulator, where the strong phase modulation imparted on a CW laser will result in a periodic chirp of the light. This means that the modulator simply varies the phase in proportion to the driving voltage, which is generally a sinusoidal electrical waveform with a frequency ω_m. Thus, the optical field of the modulator can be described as:

$$E(t) = A_0 \exp(i\omega_c t + i\Delta\phi \sin(\omega_m t)), \tag{2.6}$$

where A_0 and ω_c are the amplitude of the modulation signal and the carrier frequency. The factor $\Delta\phi$ is the so-called modulation index equal to $\pi V/V_\pi$, which relates the voltage of driving RF-signal, V, with the half-wave voltage of the modulator, V_π. The latter determines the electrical power required to achieve a π-phase change. The ratio between these two parameters must be maximized in order to achieve a broad optical spectrum. In practice, the RF power is limited and the V_π is intrinsically limited by the waveguide structure and electro-optic coefficient of the modulator.

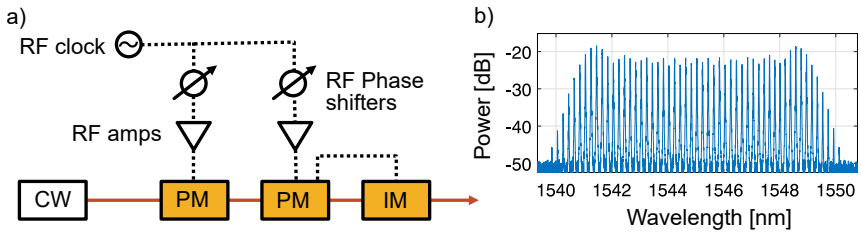

Figure 2.4: a) Electro-optic comb generation using phase and intensity modulation. The cascaded configuration of the two phase modulators (PM) increase the effective modulation depth, while the intensity modulator (IM) flattens the optical spectrum. b) Optical spectrum measured at the output.

In order to extend the optical bandwidth of the EO comb, it is common to employ a series of N phase modulators [48]. The price to pay using such a scheme is a linear increase of the optical insertion loss with each modulator. Additionally, the temporal phase between the modulators must be carefully aligned using electrical phase shifters. This EO comb configuration is depicted in Figure 2.4 a, where an additional intensity modulator is located at the output of the comb for flattening the spectrum. The intensity modulator should be biased to provide a train of pseudo-square pulses. If this temporal signal is correctly aligned with the phase of the modulators, the pulses coming out will exhibit a linear phase and hence equalize the spectrum [49]. Additional studies of the phase noise performance of these combs have shown that the comb generation in this platform is only limited to the pump laser linewidth since minimal degradation from the RF-clock purity has been found [48, 50].

Further developments to enhance this platform's capabilities are the combination with high nonlinear fibers to extend its optical bandwidth. EO combs have been spectrally broadened to bandwidths that span over an octave to enable self-referencing. In order to perform an efficient broadening, the phase noise of the comb should be controlled to maintain the coherence. Therefore, is important to consider the accumulation of phase noise with respect to the line number [51].

There are few demonstrations of self-referencing using EO combs, and it usually requires a two-stage process to realize such broadening. An initial broadening is performed mainly using a self-phase modulation mechanism operating at a low dispersion. In a second stage, the chirp of the pulse is compensated and coupled to either a fiber or waveguide that has been dispersion engineered to perform a dramatic broadening

[52,53]. In [53], the phase noise is mitigated using a microwave cavity in a stabilized-local-oscillator configuration.

2.2.2 Examples in spectroscopy

Electro-optic frequency combs stand out from other frequency comb generators because of their repetition rate tunability, high optical power handling, and stable operation. Thus, this comb generation technique rapidly gained interest for spectroscopy since they offer repetition rates in the GHz range which makes them particularly suitable for applications where dynamic measurements are needed.

EO combs have been implemented for spectroscopy using both a single and dual comb configuration. Relevant work has been reported using a single comb for molecular spectroscopy. For example, in [54] cesium transitions are probed with the pulses of an EO comb which provides a microsecond scale of measurements. Other studies on atomic spectroscopy have also benefited from the flexibility of the tuning of the line spacing to achieve rapid temporally resolved measurements [55,56].

Dual-comb spectroscopy is an established technique that allows real time measurements and comb teeth resolved spectra. This technique will be covered in more detail in Chapter 4. EO comb generators are very attractive for dual-comb spectroscopy since they significantly reduce complexity compared to MLLs-based systems. Several demonstrations for gas spectroscopy have been reported using this configuration [57–59]. Although, in some of these cases there is a large spectral sampling given by the repetition rate, the fundamental resolution is set by the comb tooth linewidth. Indeed, a vast number of demonstrations have been reported in the telecommunication bands due to the development of efficient modulators in this spectral region, this has enabled the application of spectroscopy for optical components and the characterization of waveforms [60–62].

2.3 Microcombs

Similar to EO combs, micro-resonators generate a frequency comb starting from a CW laser. However, the principle is completely different. The generation of a microcomb is based on the resonant re-circulation of light that allows to build up optical power and harness nonlinearities of the medium. A key characteristic of optical microcavities is the small spatial confinement of light which significantly reduces the threshold of

nonlinear processes [63]. They rely upon parametric gain, an amplification process that allows the generation of coherent light with a wide spectral coverage [64].

2.3.1 Generation

The Kerr-comb generation relies on the third-order nonlinearity of the material in order to observe optical parametric generation. This Kerr nonlinearity allows that two photons from the pump with a frequency ω_p generate two photons at signal and idler frequencies, named as four wave mixing (FWM). Kerr nonlinearity induced optical parametric oscillation in microcavities was first reported in [65, 66]. In these works a toroidal micro-cavity with a low high-Q allowed comb generation with low pump power. However, it was not until 2007 that frequency combs with broad optical bandwidth were demonstrated [29]. In that work, the parametric oscillation was followed by cascaded four-wave mixing, resulting in a 500 nm optical bandwidth. That demonstration not only showed wide spectral bandwidth of the generated comb, but also a constant line spacing across the spectrum [67]. The large diameter attainable in these micro-resonators platforms, opened a new venue for the generation of low noise microwave signals from optical rate frequencies [67, 68].

Besides the use of toroidal micro-cavities, the demonstration of optical parametric oscillators in integrated planar resonators was also reported [30]. The use of silicon nitride drew significant attention due to the fact that it does not suffer from two-photon absorption in the near-IR as is the case for silicon [69]. Furthermore, in [30] it was shown to be possible to fabricate thicker waveguides which enabled the waveguide dispersion to be engineered to enhance FWM processes. However, it is worth mentioning that these FWM-based microresonator combs suffer from significant frequency and amplitude noise. The later introduction of temporal dissipative solitons in [70] resulted in the formation of well-defined mode-locked waveforms, named dissipative Kerr solitons(DKS).

Similarly to optical fibre solitons, DKS relies on the balance between dispersion and non-linearities but with the extra addition of gain and loss interplay in the process [71]. The first DKS microcomb was implemented in the anomalous dispersion regime where smooth hyperbolic secant-square spectral envelopes are obtained [72]. Since this work, the investigations have focused to understand the physics driving the soliton generation and enhancing the comb capabilities. Another variant of DKS is the so-called dark soliton when the micro-resonator works

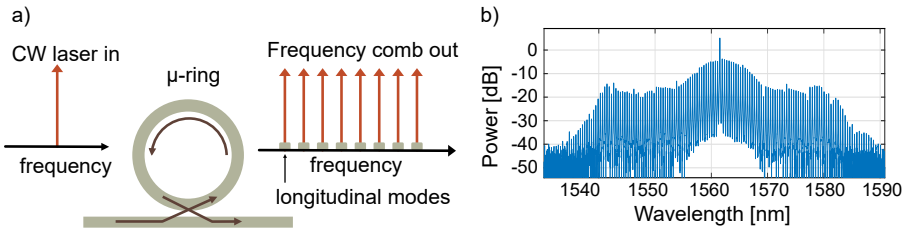

Figure 2.5: Concept of microcomb generation using a microring resonator. a) A single frequency C.W. laser is coupled to one resonance; the intracavity power builds up which allows the generation of new frequency components through nonlinear wave mixing. The repetition rate of the microcomb is governed by the free-spectral range of the cavity. b) Optical spectrum of a microcomb generated in the normal dispersion regime.

in the normal dispersion regime [73, 74]. As its name implies, it is a temporal waveform consisting of a hole in a flat background. A more detailed explanation of soliton dynamics in the normal dispersion is given in Chapter 3.

2.3.2 Examples in spectroscopy

Microcombs provide phase-locked femtosecond pulses with reproducible spectral envelopes and good phase noise characteristics. Furthermore, Kerr microcombs unleashed the potential of increased bandwidth that is possible to extend up to an octave spanning [75]. Chip-based frequency combs represent an opportunity for a myriad of outside laboratory applications to reduce component size and complexity [76–80]. Coherent microcombs have enable its application on imaging, tomography and ranging [31, 32, 34].

Undoubtedly, microcombs are also very appealing for optical spectroscopy. Direct frequency comb spectroscopy has been demonstrated using a scanning technique to increase the effective resolution [81, 82]. Dual-comb spectroscopy is an established technique due to its performance capabilities in terms of SNR and fast measurements. Therefore, the use of microcombs has been very attractive to implement this configuration [33, 83–85]. A more thorough study of the performance of dual-comb on chip is given in Chapter 4.

Chapter 3

Photonic-chip-based combs in the normal dispersion regime

The generation of frequency combs on integrated photonic chips is an enabling technology in the field of nonlinear photonics. Photonic devices implemented within square millimeter areas are capable to provide high confinement which is essential for nonlinear optics. Furthermore, they enable the possibility of tailoring the dispersion profiles of the waveguides to further enhance the nonlinear parametric processes.

In connection with the results presented in paper A and B, this chapter is mainly focused on the generation of nonlinear broadening and microcomb generation in the normal dispersion regime.

3.1 Nonlinear optics in waveguides

A variety of material platforms have been employed to fabricate waveguides for nonlinear applications, including silicon [86, 87], silicon nitride [88–90], AlGaAs [91], and AlN [92]. Si_3N_4 has the advantage that it offers a wide transparency window and high nonlinear coefficient, and does not exhibit nonlinear losses such as two-photon absorption.

The generation of broad spectra on chip-based combs is mainly supported by supercontinuum (SC) generation using optical waveguides and Kerr comb generation based on microresonators [93]. In both cases, the governing nonlinear mechanisms are different depending on the dispersion regime of operation. This results in different combinations between the spectral broadening bandwidth and the coherence that is possible to obtain [94].

A key difference between SC and Kerr comb generation is that the former utilizes a pulse as the pump source, while the latter is pumped with a CW laser. In SC generation, a pulse propagates through an optical waveguide that features either anomalous or normal dispersion, resulting in different nonlinear broadening mechanisms [94]. Since the pulse that is used as the pump is a frequency comb itself, the repetition rate of the broadened spectra is dictated by the input pulse. For the case of Kerr combs, the CW laser is coupled to one of the microresonator resonances transferring energy to other cavity modes via FWM where the repetition rate is given by the FSR of the microresonator.

Integrated waveguides offer the possibility to achieve a high confinement of light due to the large contrast of the refractive index between the core and the cladding. High confinement and dispersion engineering can be obtained by tailoring the waveguide geometry. The combination of these two properties is key for enabling nonlinear optics processes [95]. The propagation length is another essential parameter for nonlinear processes.

Since the pulse propagates through a guided mode of the waveguide, we have to account for propagation constant β which is frequency dependent. The dispersion in the optical mode is caused by two contributions, material and waveguide dispersion. The propagation constant is commonly expressed as a Taylor expansion.

$$\beta(\omega) = \beta_0(\omega_0) + \beta_1(\omega - \omega_0) + \sum_{n=2}^{\infty} \frac{\beta^n}{n!}(\omega - \omega_0)^n, \tag{3.1}$$

where β_n corresponds to an nth-order derivative with respect to an angular frequency ω_0, β_1 is related to the group velocity $\nu_g = 1/\beta_1$. The second-order derivative β_2 defines the group velocity dispersion (GVD) coefficient. When $\beta_2 > 0$, the waveguide has normal dispersion, meaning that the low-frequency components travel faster than the high-frequency components and vice versa for anomalous dispersion which occurs when $\beta_2 < 0$. Although dispersion is a linear phenomenon, its influence on the nonlinear interactions of the waveguide is extremely important. This since the different velocities on the spectral components of the pulse will affect the phase-matching condition in the spectral broadening.

In order to describe the propagation of a pulse through a Kerr nonlinear waveguide, we use the nonlinear Schrödinger equation (NLSE) [96]. This equation is relatively simple to simulate using a split-step method approach, where the propagation is considered in small steps taking sep-

arately the linear and nonlinear terms of the NLSE.

$$\frac{\partial A}{\partial z} = -\frac{\alpha}{2}A + \frac{i\beta_2}{2}\frac{\partial^2 A}{\partial t^2} + i\gamma|A|^2 A. \tag{3.2}$$

In the NLSE, the change of the slowly varying electric field envelope (A) with respect to the propagation distance is related to the Kerr nonlinear effect, the GVD, and the propagation losses, as seen on the right side of Equation 3.3 respectively. For simplicity, only the second-order dispersion is considered in the simulation using co-moving frame at the group velocity. The Kerr nonlinearity in the NLSE is represented by the nonlinear parameter γ, which causes a change in the refractive index of the mode resulting in an intensity dependant phase.

3.2 SC generation in the all-normal dispersion regime

It is clear that in order to describe the evolution of a pulse in a nonlinear medium, the dispersion and the nonlinearity must be examined together. In the case where the waveguide features normal dispersion, the combination of GVD and SPM produces a broadening of both the spectrum and the pulse. In the presence of anomalous dispersion, the nonlinear frequency chirp is balanced with the GVD which in turn enables the generation of solitons. Indeed, soliton-induced dispersive wave generation represents an efficient option for SC generation. However, these processes rely on a region of parametric gain called modulation instability (MI).

A limitation of this method is that unseeded MI-gain can amplify the noise of the input pulse [97]. For this reason, pump pulses with a duration shorter than 200 fs are needed.

An alternative for coherent SC generation is working in the all-normal dispersion (ANDi) regime. Although the employment of ANDi fibers has been studied as an alternative for the conventional SC generation, its realization on integrated waveguides is still challenging. There are two key aspects for the realization of nonlinear broadening in the ANDi regime. First, since the maximum broadening is governed by the initial SPM, the pulse should not broaden immediately. Therefore, the GVD should be as low as possible to keep a high peak power. Second, since the OWB distance grows with the duration of the pulse, the propagation distance should be large enough.

By working in the ANDi regime, all soliton dynamics are suppressed. Instead, the dominant nonlinear dynamics are SPM and optical wave breaking (OWB) [98]. In figure 3.1, a simulation of SC generation in the anomalous and the normal dispersion regime is depicted. In the conventional case, an anomalous dispersion waveguide is pumped with a 60 femtosecond pulse at a peak power of 1 kW. The spectral evolution illustrates that the spectral broadening is induced by a soliton until it breaks apart after a propagation around 30 mm. This is caused by the presence of higher-order dispersion which in turn generates a dispersive wave that enhances the broadening [99]. As a result, the output spectrum exhibits a complex structure with large dips which is undesirable for many applications. The ANDi waveguide is also simulated with the same pulse but at higher peak power (4 kW). At the initial stage of the pulse propagation, the spectral broadening is mainly produced by SPM as the characteristic oscillatory structure in the spectrum is observed. In the temporal domain, the pulse maintains its shape and broadens from its initial duration. The reason for the nonlinear dynamics in this case, where SPM is being dominant over the dispersion, is because the nonlinear length $L_{NL} = (\gamma P_0)^{-1}$ is shorter than the propagation $L_D = T_0^{-1}/|\beta_2|$. Here T_0 and P_0 are the duration and peak power of the initial pulse. After a longer propagation, the dispersion takes over the nonlinear dynamics. This occurs due to the fact that the group velocity increases monotonically since all wavelengths exhibit normal dispersion. As a result, the trailing and leading edges of the pulse are steepened and OWB occurs. This temporal overlap of the pulse frequency components translates into the creation of new frequency components via four-wave mixing [100].

As the pulse propagates further, OWB tranfers energy from the central frequency region to the edges, causing a flattening of the spectrum. Therefore, the maximum achievable bandwidth mainly depends on the SPM-induced broadening, which is defined as [96]

$$|\omega_{SPM}(z,t) - \omega_0| = \gamma P_0 \frac{\partial U(t)}{\partial t} z, \tag{3.3}$$

where U(t) is the normalized intensity of the pulse and z is the propagation distance.

Due to the temporal overlapping of the spectral components of the pulse, OWB is highly sensitive to the input pulse characteristics. In paper A, the ANDi waveguide was pumped using a femtosecond MLL, this was performed in free space to avoid the initial pulse broadening

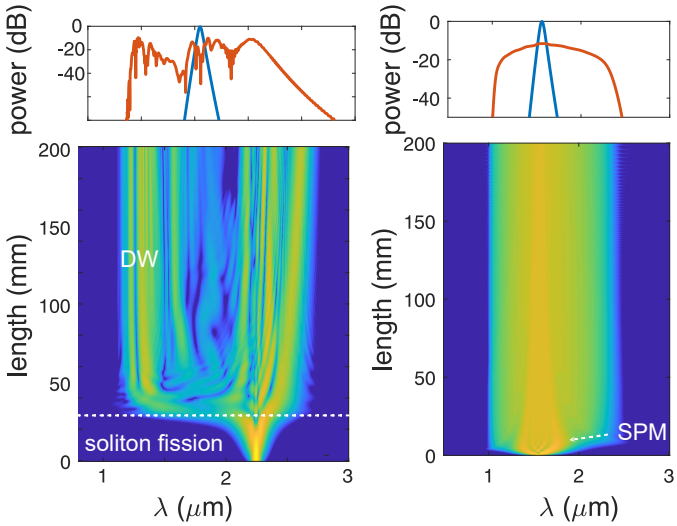

Figure 3.1: Spectral evolution of the SC generation in anomalous and normal dispersion. In the left, an anomalous dispersion waveguide is pumped with a 60 fs pulse at 1kW. A pulse with the same duration but 4 kW of optical power is used to simulate the nonlinear process in an ANDi waveguide. The top panels depict the spectrum of the input pulse and the SC generated after 20 cm of propagation.

prior to propagation. This ensures a high peak power, however, due to the nonlinearities of the built-in amplifiers of the system, the pulse of the laser shows a complex structure which is translated to the broadened spectrum.

In paper A, supercontinuum generation using ANDi waveguides was studied. In this work, the influence of the pulse duration and the coherence of the broadened spectrum was analyzed. This offers an alternative to bulky optical components for the generation of frequency combs on-chip with high repetition rates and a flat spectral envelope. These characteristics are not only beneficial for spectroscopy but also for noise-sensitive applications such as communications and arbitrary waveform synthesis.

3.3 Mode-locked Kerr microcombs

Another approach to implement an integrated frequency comb is the microresonator-based Kerr comb [101]. The main component is a nonlinear optical microresonator based on a third order nonlinear material with a high quality factor (Q). The basic configuration consist of a microresonator coupled to a bus waveguide, when a single-frequency CW laser is coupled to the resonator a frequency comb is generated through nonlinear four-wave mixing. Mode-locking is attainable in microcombs by operating in the soliton regime, where the CW laser is converted into stable ultrashort pulses in time domain [72,73,102–104]. Similarly to the SC generation, the group velocity dispersion inside the microresonator plays an important role for the microcomb formation. The spectrum of a microcomb generated when operating in the anomalous dispersion and a mode-locked dark comb is shown in Figure 3.2

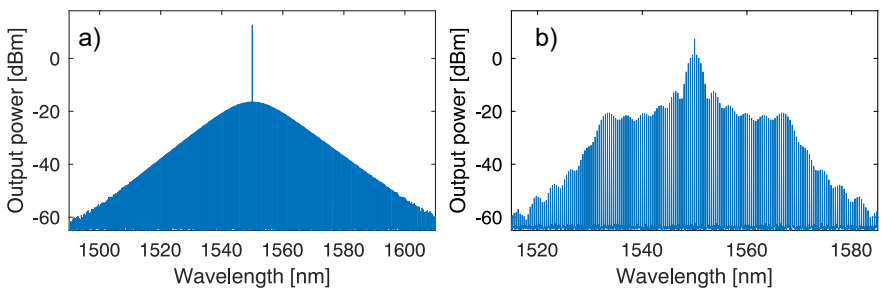

Figure 3.2: Kerr microcombs. a) A bright soliton featuring a hyperbolic spectral envelope is generated in a microresonator with anomalous dispersion. b) shows the spectrum of a dark pulse when the cavity dispersion is normal.

The processes occurring in nonlinear microcavities can be divided in two stages. The first one is modulation instability, where new equally spaced frequency components are generated. In the second second stage, complex nonlinear dynamics including sub-comb formation and breathing states lead to comb formation [103]. For the initial growth of optical frequencies, it is necessary to access the modulation instability, which occurs when the CW field of power provides parametric amplification to other frequency components. When the gain compensates for the cavity losses, new frequency components are generated in the resonances of the cavity.

Mode-locking in the normal dispersion regime have been demonstrated theoretically and experimentally [73, 74, 105]. The comb generation in this regime is quite attractive for several reasons, one of them is due to the fact that the dispersion of several bulk materials is normal in the visible and near IR spectral windows. Indeed, in the telecommunications band, where Kerr comb generation has mainly been performed, it is possible to tailor the dispersion of the waveguide since most of the materials exhibit either zero-dispersion crossing, or low anomalous/normal dispersion. Nevertheless, operating in the normal dispersion relaxes the requirement of dispersion engineering, which is desirable to conform other requirements for Kerr comb generation, such as mode confinement and high Q factors. Other interesting aspects of the Kerr comb formation in the normal dispersion region are the deterministic behaviour towards mode-locking and the high conversion efficiency [106–108].

The resonances in the microresonator are defined by the free-spectral range (FSR) of the ring and the group velocity dispersion. If the GVD of the fundamental mode of the microresonator is designed to operate in the normal dispersion region, the blue frequency components travel slower than the red ones. This means that the spacing between the resonances decreases as the frequency increase.

A useful tool to model the dynamics of a microresonator with length L and intrinsic propagation losses α, is the Lugiato-Lefever equation [109]. This equation is also known as the externally driven, damped nonlinear Schrödinger equation, due to the presence of an external driving field A_{in} with detuning.

$$T_R \frac{\partial A}{\partial t} = \left[\frac{\theta + \alpha L}{2} - i\delta_0 - iL\frac{\beta_2}{2}\frac{\partial^2}{\partial \tau^2} + iL\gamma|A|^2 \right] A + i\sqrt{\theta} A_{in}, \tag{3.4}$$

where T_R is the roundtrip time in the microresonator, A is the intracavity field, θ is the coupling coefficient between the bus waveguide and the ring, δ_0 is the detuning parameter of the cavity resonance from the pump frequency and A_{in} is the incident pump field.

The initiation of Kerr microcomb in normal DKS is experimentally challenging because of the difficulty to access the MI to grow the first comb lines. Although it is well known that MI existence requires anomalous dispersion in fibers, the MI in cavities may arise in both anomalous and normal dispersion [110]. In optical fibers, MI has been observed when a field interacts with another field with different polarization or wavelength [96].

In optical microresonators, the mode interaction between the trans-

verse and fundamental mode enables a localized anomalous dispersion which allows MI to occur [73, 74, 104]. These aided coupling interaction is however a product of accidental degeneracies in the spatial modes in the microresonator, making it difficult to control. This issue can be addressed by using a second cavity to induce the mode coupling, in this manner it is possible to control the coupling juts by tuning the distance between the two rings. This was proposed in [107] where a dual-coupled ring arrangement induces mode coupling in a programmable way. Besides achieving mode-locking deterministically, the repetition rate of the comb can be selected by controlling the mode interaction location. A similar approach was performed in [108] where a microheater is placed on the auxiliary cavity to tune the avoided mode crossing location.

Mode-locked pulses generated in the normal dispersion regime, also called dark solitons, enable high power conversion efficiency [106–108]. Efficiency higher than 30 percent can be achieved due to the fact that the CW laser is detuned closer to the center of the resonance of the microresonator. For the generation of bright solitons in the anomalous dispersion regime, the pump CW laser is far red-detuned from the resonator resonance. Due to this large frequency detuning, a smaller portion of the CW laser power is coupled to the resonance and causes just a fraction to be converted into usable comb power. However, a recent work demonstrates that this limitation can be overcome by using a dual cavity architecture to induce a frequency shift of the pump resonance, this in turn allows an unprecedented conversion efficiency [111].

In paper B, the experimental investigation of a microcomb in a dual-cavity configuration operating the normal dispersion is performed. The frequency comb attains a power conversion efficiency of 50 percent and a repetition rate of 50 GHz. The design of this dual-cavity design is similar as in [111], where the main cavity has a larger FSR than the auxiliary cavity. This enables a mode-crossing in a single resonance, enabling a symmetric spectral envelope and a resilience of the repetition rate to the pump frequency detuning.

Chapter 4

Dual-comb interferometry

An optical frequency comb is an exceptional tool for spectroscopy due to its brightness and spatial and temporal coherence. In order to fully exploit their spectral resolution and frequency accuracy, it is needed to resolve the individual comb teeth. Measuring comb-tooth-resolved spectra represents a challenge since the separation of individual frequency lines is finer than the resolution of most spectrometers. In paper C, a review of comb-based interferometric techniques are presented. This section focuses on dual-comb interferometry and the possibility to employ chip-scale microcombs for this purpose.

4.1 Comb-based interferometry in the time domain

The use of frequency combs for optical spectroscopy within linear interferometric techniques has been widely explored over the recent years [112]. The simplest method for employing the broad bandwidth of a comb is direct frequency comb spectroscopy (DFCS). This technique has found a myriad of applications in molecular spectroscopy, material science, and trace gas detection. It was rapidly realized that without the capability to fully resolve the comb lines, the associated frequency resolution was lost. Indeed, fully resolved comb spectra using dispersive and Fourier-transform (FT) spectrometers has been achieved [4, 113].

Fourier transform spectroscopy (FTS) is a well-established technique capable of recording a full spectrum over a wide spectral bandwidth using broadband thermal sources as the input. Fourier transform spectrometers have been implemented using frequency combs as the input source,

consequently increasing the SNR due to their excellent spatial coherence [4]. Although the sensitivity was increased, the initial implementation did not fully resolve the spectral lines since it was limited by the instrumental resolution given by the maximum path length of the interferometer. However, recent demonstrations of frequency combs coupled to FT spectrometers fully resolve the comb teeth linewidth by matching the comb repetition rate with the delay of the spectrometer [114, 115]. Combined with enhancement cavities, the sensitivity is further increased due to a longer interaction path of the sample [116, 117].

As with conventional FT spectroscopy, dual-comb spectroscopy (DCS) enables the broad bandwidth optical sampling without the need of movable components but instead using a dual-comb configuration. In this way, two combs with different repetition rates allow mapping of the optical frequencies into the photo-detectable radio frequency domain. Using this technique, the second frequency comb is used to perform the spectral sampling and therefore dispense the need for a spectrometer [59, 118, 119]. Dual comb spectroscopy (DCS) has outpaced other comb spectroscopy techniques since it brings together the strengths of broadband spectroscopy and laser spectroscopy. DCS has been widely used to perform direct frequency comb spectroscopy using MLLs in the near-IR and in the mid-IR [3, 120–122]. However, it is important to remark that in the mid-IR the complexity of the DCS increases since most of the mid-IR implementations require nonlinear conversion methods.

DCS is analogous to Fourier-transform infrared (FTIR) spectroscopy, where broad bandwidth spectra is measured with a single photodetector. Although FTIR spectroscopy is very unlikely to be surpassed in terms of spectral coverage, other features such as spectral resolution and accuracy are possible to attain using a comb-based approach. Notwithstanding, the development of DCS largely mirrors the growth of frequency comb generation. The advent of microcombs has opened up the possibility of using frequency combs for integrated spectroscopy leveraging high SNR and fast acquisition rates. The outstanding phase noise characteristics in recent microcomb demonstrations make them even more appealing for DCS applications. However, the stabilization of microcombs is a key aspect to reach the fundamental resolution of DCS which is set by the linewidth of the comb tooth.

4.2 Generalities of dual-comb interferometry

Dual-comb was proposed shortly after the invention of the frequency comb by Schiller et all [123], and since then it has been established and evolved alongside the frequency comb technology. As mentioned earlier, DCS uses two frequency combs whose repetition rate have a slight frequency difference Δf_{rep} (see figure 4.1 (a,b)). The main idea is that these two combs interfere and generate a frequency comb in the RF domain composed of the heterodyne beating of the frequency comb lines. In the RF domain, the sequence of beat notes is spaced by the difference of the repetition rate Δf_{rep}. In Figure 4.1 (b), the general idea of this concept is depicted. In the time domain, DCS can be understood as two trains of pulses with slightly different repetition rates, overlapping at the photodetector with varying delays. The photodetected cross-correlation is then sampled at time intervals $\Delta T = 1/f_{rep}$, as shown in figure 4.1 (c).

In order to perform spectroscopy, a sample under test is placed in one of the arms of the dual-comb interferometer. In this way, the response of the sample is encoded in the so-called signal comb and then sampled by the second comb, which is referred to as the local oscillator. This scheme allows to retrieve both the amplitude and phase of the sample and is often called asymmetric or dispersive architecture [118]. Using a symmetric approach is also possible, where the two combs interact with the sample, but only the amplitude of the comb, i.e absorption features, are measured. In the following, the asymmetric approach will be considered.

Dual-comb spectroscopy is sometimes described in terms of electric-field cross-correlation (EFXC). In [61], this scheme was proposed for the characterization of optical arbitrary waveforms. It is possible to draw an analogy with traditional EFXC, where the cross-correlation between a signal pulse (a_s) and a reference pulse (a_r) is measured with respect to the delay (τ) of an interferometer. This delay is controlled by the mechanical translation of one of the arms of the interferometer. The interference is then recorded by a photo-detector yielding a time-averaged output power as in [124].

$$\langle P_{out}(t)\rangle = \frac{1}{2}\{U_r + U_s + [e^{j\omega_0\tau}\langle a_s(t)a_r^*(t-\tau)\rangle + c.c]\} \tag{4.1}$$

Where U_r and U_s are the energies of the pulses, these terms will correspond to DC components in the photo-detection. The oscillatory

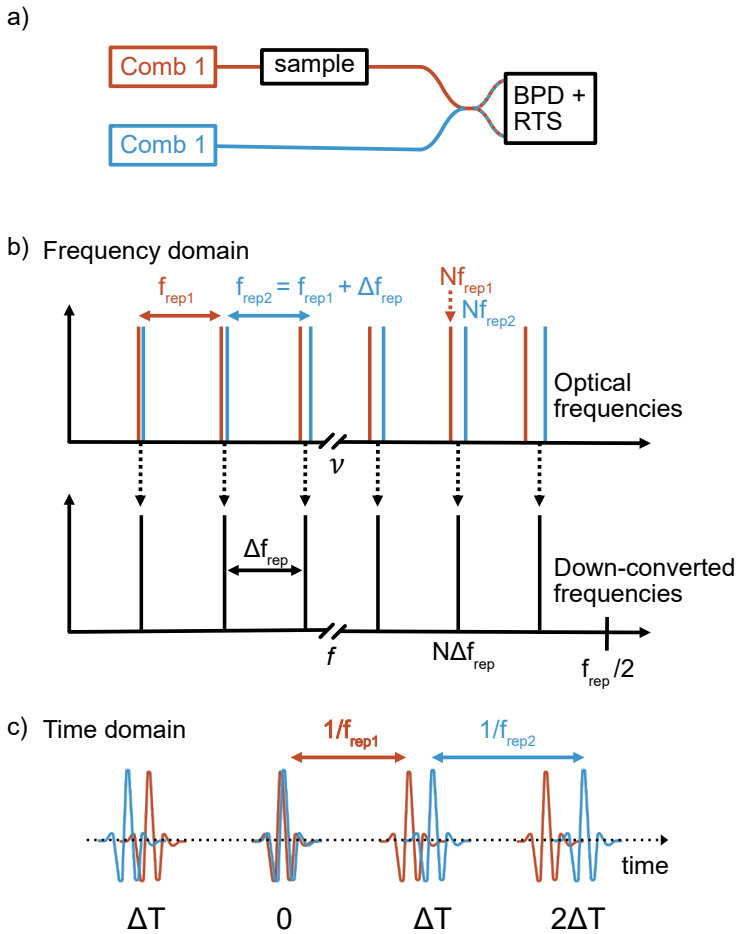

Figure 4.1: a) The basic setup of a dual-comb interferometer in an asymmetric architecture. b) Two frequency combs (red and blue) are mixed to produce a down-converted rf comb. c) In time-domain, a pulse-to-pulse walk-off between the two comb pulse trains is produced, i.e. a virtual scanning of a reference pulse over a signal pulse. The samples are recorded by a balanced photodetector (BPD) at time intervals of ΔT using a real-time scope (RTS).

term measured as a function of the delay τ, contains the information of the sample under test. Through Fourier analysis, it is possible to retrieve the signal pulse if the reference pulse is known.

The same approach can be used in dual-comb interferometry, but instead, the delay is controlled by the difference of the repetition rate of the two combs. Therefore, the local oscillator pulse virtually scans the

signal pulses, producing a cross-correlation interferogram with a period $1/\Delta f_{rep}$, as depicted in Figure 4.1(b).

Therefore, the Fourier transformation of the product of the electric field of both combs will simply translate to a radio-frequency comb. Since the difference of the repetition rate is the separation of the frequency lines of the RF domain, the bandwidth of the RF comb should not exceed half of the repetition rate. This is derived from the Nyquist condition and is maintained if the optical spectral bandwidth that is desired to acquire fulfills the following condition [118]:

$$\Delta\nu < \frac{m f_{rep}}{2} = \frac{f_{rep}^2}{2\Delta f_{rep}} \tag{4.2}$$

Where m is the so-called compression factor equal to $f_{rep}/\Delta f_{rep}$. If Δf_{rep} increases, the down-converted bandwidth will also increase, which will translate in aliasing. This means that increasing the difference in repetition rate beyond this limit, the down-converted frequencies will expand and overlap with beating of higher order frequencies. From equation 4.2, the maximum difference in repetition rate can be expressed as

$$\Delta f_{rep} = \frac{f_{rep}^2}{2\Delta\nu} \tag{4.3}$$

In terms of acquisition speed, the minimum time needed to acquire a single spectrum using DCS is given by $1/\Delta f_{rep}$ at the expense of low SNR. One can realize that fast spectral acquisition is possible by increasing the difference in the repetition rate. Furthermore, as seen in equation 4.3, the acquisition speed scales with the repetition rate.

The SNR can be further increased by co-adding multiple successive spectra, i.e coherent averaging. Therefore, improved SNR can be obtained without the need for long measurement acquisition times if an ultrafast single acquisition speed is performed. This scheme has been implemented using electro-optic combs [59–61,125] or microcombs whose repetition rates are usually in the order of GHz [34].

4.3 Microcombs for dual-comb interferometry

As mentioned above, in order to avoid aliasing effects $f_{rep} > \Delta f_{rep}$ must be satisfied. Microcombs are appealing to fulfill this condition since their

repetition rates (in GHz) enable faster measurements than their counterparts based on mode-locked lasers (in MHz). However, the challenges associated to perform dual-comb spectroscopy using microcombs mainly lie on the lack of mutual coherence if they are generated with different lasers. If both microresonators are pumped with a single CW laser, another practical aspect rises since the resonances of both microresonators should be aligned.

The mutual coherence is highly relevant in order to spectrally resolve the comb teeth, this means that the down-converted linewidth should be below Δf_{rep}. Another aspect is the possibility of performing long-term averaging which in turn increases the SNR. In this matter, new methods have been explored to achieve inherent mutual coherence and reducing the experimental complexity. One of these approaches is based on the generation of microcombs in the same cavity, either in a counter-propagation architecture [83–85]. However, this technique relies on Kerr and Raman effect to induce the difference in the repetition rate [126] which restricts the acquisition speed. A recent demonstration pumping with a single laser employs spatial multiplexing [127] to generate frequency combs in different mode families, which enables repetition rate differences in the MHz range.

Simultaneous generation of frequency combs is also possible using a single laser pumping two cavities on a single chip [33]. In this approach, the presence of microheaters on top of the cavities allows to thermally tune the resonance of the cavity to achieve soliton mode-locking. Hence, it is possible to use low-noise non-tunable lasers, leading to a narrow linewidth of the down-converted beat notes and stable mutual coherence. It also overcomes the challenge of aligning the resonances to the same pump wavelength since the tunability of the heaters can be up to one FSR. It is worth mentioning that since the central wavelength is shared, an ambiguity in the beating of the closer lines to the pump is observed. This can be avoided using an acousto-optic modulator but it requires a different bus waveguide to pump the rings. This is difficult in practice since the devices are usually pumped using individual lensed fibers on a thermally controlled micro-positioned stage. Packaging of microresonators for external pumping would increase the flexibility of the microcomb generation and also leverages a stable power coupling [128, 129].

The most straightforward application of a dual-comb scheme based on microcombs, is the observation of the comb formation dynamics

[33, 127]. The fast recording of the interferometric data between a reference comb and a comb in formation allows to spectrally resolve the comb dynamics. Such imaging was initially demonstrated in [130] using an electro-optic comb as the reference pulse to sample a dissipative Kerr soliton formation. The temporal resolution in the femtosecond scale allowed for observation of soliton phenomena such as collision and breathing, this resolution is fundamentally limited by the pulse duration of the reference. The EO-comb can be replaced by another microcomb which will allow for higher sampling rates, evidently a stable mode-locking operation state of both combs is needed in order to resolve the individual comb lines beating.

Chapter 5

Future outlook

The work presented in this thesis has been focused on the generation of microcombs. A natural next step would be to work with the application of microcombs in optical spectroscopy, specifically in a dual-comb configuration.

5.1 Static dual-comb spectroscopy on chip

The work presented in paper B is a preliminary study of the microcomb generation in the normal dispersion regime. It is worth mentioning some important aspects about this work such as the flat and symmetric spectral envelope, high power conversion efficiency and the presence of a quiet point operation. These capabilities are attractive for the usage of this type of comb in a dual-comb interferometry scheme. As mentioned in chapter 4, this scheme brings benefits such as increased SNR and fast dynamic measurements. However, it is required to achieve a mutual coherence between the combs and a stable repetition rate to fully resolve the comb teeth. A mutual coherence can be achieved using the same CW laser as the pump.

The drifting of the repetition rate is more challenging to overcome since it requires an active feedback stabilization. The thermal stabilization of the cavity can be implemented by monitoring the generated optical spectrum and using the heater on the main cavity to compensate the drifting. To achieve better stabilization is important to disentangle the contributions on the phase of the repetition rate to distinguish between the thermal noise of the cavity and the noise from the laser.

In order to perform dual-comb spectroscopy it is crucial to overcome

these practical aspects on the frequency comb generation. Nevertheless, the use of dark soliton microcombs is remarkable since it make it possible to achieve a higher dynamic range of detection as a result of the symmetry of these combs.

5.2 Combination of DCS with swept-wavelength interferometry

The spectral resolution attainable with DCS is fundamentally limited by the linewidth of the comb teeth. However, the spectral sampling is given by the repetition rate of the frequency comb. This spacing, which is typically in hundreds of GHz for microcombs, can be overcome with the combination of swept-wavelength interferometry. Using such approach, the common pump laser is swept over the repetition rate span, which in turn reduce the resolution to narrower than the comb linewidth.

The challenge of implementing the sweeping of the pump laser lies in maintaining a constant detuning between the laser and the pump resonance. This means that it is needed to tune the resonance of the main cavity over the full FSR of the comb while keeping a mode-locked state. If a dual cavity architecture is used for the initiation, it also requires tuning the auxiliary cavity resonance in order to maintain the avoided mode-crossing needed for the comb generation.

The key feature of realizing such task, is combining the high spectral resolution of swept-wavelength interferometry with a broad bandwidth frequency comb. Ideally, by using this technique it is possible to perform high resolution spectroscopy over octave-spanning frequency combs. Applied to molecular spectroscopy, this would imply the massive characterization in parallel of multiples species.

Chapter 6

Summary of Papers

Paper A

Coherent supercontinuum generation in all-normal dispersion Si_3N_4 waveguides,
Optics Express, 30, 8641-8651, 2022.

In this paper we study the coherence properties of supercontinuum generation using straight waveguides in the normal dispersion regime. The spectrum of sub-picosecond pulses from an electro-optic comb with a high repetition rate is broadened by means of self-phase modulation in the normal dispersion. Pulses with higher energy with a femtosecond duration are also used as a pump source to access the optical wave-breaking regime.

My contributions: I assisted in the design of the waveguide and conducted the characterization of different samples. I conducted all the lab experiments including pumping the waveguide with different pulses and the coherence characterization of the broadened spectra. I wrote the paper with support from the co-authors and presented the work at CLEO EU 2021.

Paper B

Photonic molecule microcombs at 50 GHz repetition rate,
Conference on Lasers and Electro-Optics, San Jose, USA, paper SW4O.8, 2022

In this work, we demonstrate the generation of a frequency comb in the normal dispersion regime using a dual-cavity architecture. We address the challenge of comb initiation in the normal dispersion regime by inducing mode coupling by means of an auxiliary cavity. An important aspect in the design of this dual-cavity architecture is that the main cavity has a larger FSR than the auxiliary cavity. In this way, the avoided mode-crossing is only induced on a single resonance. As a consequence, the generated comb results in a symmetric envelope and the presence of a quiet point of operation is observed.

My contributions: I conducted the lab experiments and presented the work at CLEO 2022.

Paper C

Frequency-comb-based spectral interferometry for characterization of photonic devices,
Micromachines, 13, no 4, p. 614, 2022.

We present an state of the the art concerning the use frequency combs for spectral interferometry. The benefits leveraged by frequency combs are discussed using different interferometry configurations.

My contributions: I wrote the sections that describe the techniques of time and spectral domain and a sub-section of the applications. I assisted in the preparation of the complete manuscript.

References

[1] N. C. Thomas, "The early history of spectroscopy," *Journal of chemical education*, vol. 68, no. 8, p. 631, 1991.

[2] M. N. Fiddler, I. Begashaw, M. A. Mickens, M. S. Collingwood, Z. Assefa, and S. Bililign, "Laser spectroscopy for atmospheric and environmental sensing," *Sensors*, vol. 9, no. 12, pp. 10 447–10 512, 2009.

[3] F. Adler, P. Masłowski, A. Foltynowicz, K. C. Cossel, T. C. Briles, I. Hartl, and J. Ye, "Mid-infrared Fourier transform spectroscopy with a broadband frequency comb," *Opt. Express*, vol. 18, no. 21, pp. 21 861–21 872, 2010.

[4] J. Mandon, G. Guelachvili, N. Picqué, F. Druon, and P. Georges, "Femtosecond laser Fourier transform absorption spectroscopy," *Optics Letters*, vol. 32, no. 12, pp. 1677–1679, 2007.

[5] E. V. Loewenstein, "The history and current status of Fourier transform spectroscopy," *Applied Optics*, vol. 5, no. 5, pp. 845–854, 1966.

[6] P. Edwards, C. Zhang, B. Zhang, X. Hong, V. K. Nagarajan, B. Yu, and Z. Liu, "Smartphone based optical spectrometer for diffusive reflectance spectroscopic measurement of hemoglobin," *Scientific Reports*, vol. 7, no. 1, pp. 1–7, 2017.

[7] E. Ryckeboer, R. Bockstaele, M. Vanslembrouck, and R. Baets, "Glucose sensing by waveguide-based absorption spectroscopy on a silicon chip," *Biomed. Opt. Express*, vol. 5, no. 5, pp. 1636–1648, 2014.

[8] A. J. Das, A. Wahi, I. Kothari, and R. Raskar, "Ultra-portable, wireless smartphone spectrometer for rapid, non-destructive testing of fruit ripeness," *Scientific reports*, vol. 6, no. 1, pp. 1–8, 2016.

[9] Z. Yang, T. Albrow-Owen, W. Cai, and T. Hasan, "Miniaturization of optical spectrometers," *Science*, vol. 371, no. 6528, p. eabe0722, 2021.

[10] A. J. McGonigle, T. C. Wilkes, T. D. Pering, J. R. Willmott, J. M. Cook, F. M. Mims, and A. V. Parisi, "Smartphone spectrometers," *Sensors*, vol. 18, no. 1, p. 223, 2018.

[11] N. Alshamrani, A. Grieco, B. Hong, and Y. Fainman, "Miniaturized integrated spectrometer using a silicon ring-grating design," *Optics Express*, vol. 29, no. 10, pp. 15 279–15 287, 2021.

[12] O. Schmidt, P. Kiesel, and M. Bassler, "Performance of chip-size wavelength detectors," *Optics Express*, vol. 15, no. 15, pp. 9701–9706, 2007.

[13] M. C. Souza, A. Grieco, N. C. Frateschi, and Y. Fainman, "Fourier transform spectrometer on silicon with thermo-optic non-linearity and dispersion correction," *Nature communications*, vol. 9, no. 1, pp. 1–8, 2018.

[14] A. Nitkowski, L. Chen, and M. Lipson, "Cavity-enhanced on-chip absorption spectroscopy using microring resonators," *Opt. Express*, vol. 16, no. 16, pp. 11 930–11 936, 2008.

[15] S. Nezhadbadeh, A. Neumann, P. Zarkesh-Ha, and S. Brueck, "Chirped-grating spectrometer-on-a-chip," *Optics Express*, vol. 28, no. 17, pp. 24 501–24 510, 2020.

[16] B. Gao, Z. Shi, and R. W. Boyd, "Design of flat-band superprism structures for on-chip spectroscopy," *Opt. Express*, vol. 23, no. 5, pp. 6491–6496, 2015.

[17] G. Micó, B. Gargallo, D. Pastor, and P. Muñoz, "Integrated optic sensing spectrometer: Concept and design," *Sensors*, vol. 19, no. 5, 2019.

[18] P. Cheben, J. H. Schmid, A. Delâge, A. Densmore, S. Janz, B. Lamontagne, J. Lapointe, E. Post, P. Waldron, and D.-X. Xu, "A

high-resolution silicon-on-insulator arrayed waveguide grating microspectrometer with sub-micrometer aperture waveguides," *Opt. Express*, vol. 15, no. 5, pp. 2299–2306, 2007.

[19] B. Momeni, E. S. Hosseini, and A. Adibi, "Planar photonic crystal microspectrometers in silicon-nitride for the visible range," *Opt. Express*, vol. 17, no. 19, pp. 17 060–17 069, 2009.

[20] X. Nie, E. Ryckeboer, G. Roelkens, and R. Baets, "CMOS-compatible broadband co-propagative stationary Fourier transform spectrometer integrated on a silicon nitride photonics platform," *Optics Express*, vol. 25, no. 8, pp. A409–A418, 2017.

[21] D. M. Kita, B. Miranda, D. Favela, D. Bono, J. Michon, H. Lin, T. Gu, and J. Hu, "High-performance and scalable on-chip digital fourier transform spectroscopy," *Nature Communications*, vol. 9, no. 1, pp. 1–7, 2018.

[22] A. V. Velasco, P. Cheben, P. J. Bock, A. Delâge, J. H. Schmid, J. Lapointe, S. Janz, M. L. Calvo, D.-X. Xu, M. Florjańczyk *et al.*, "High-resolution fourier-transform spectrometer chip with microphotonic silicon spiral waveguides," *Optics Letters*, vol. 38, no. 5, pp. 706–708, 2013.

[23] M. Nedeljkovic, A. V. Velasco, A. Z. Khokhar, A. Delâge, P. Cheben, and G. Z. Mashanovich, "Mid-infrared silicon-on-insulator fourier-transform spectrometer chip," *IEEE Photonics Technology Letters*, vol. 28, no. 4, pp. 528–531, 2015.

[24] S. Svanberg, "Laser spectroscopy applied to energy, environmental and medical research," *Applied Physics B*, vol. 46, no. 3, pp. 271–282, 1988.

[25] R. Bell, *Introductory Fourier transform spectroscopy.* Elsevier, 2012.

[26] J. L. Hall, "Nobel Lecture: Defining and measuring optical frequencies," *Reviews of Modern Physics*, vol. 78, no. 4, pp. 1279–1295, 2006.

[27] T. W. Hänsch, "Nobel lecture: Passion for precision," *Reviews of Modern Physics*, vol. 78, no. 4, pp. 1297–1309.

[28] A. Pasquazi, M. Peccianti, L. Razzari, D. J. Moss, S. Coen, M. Erkintalo, Y. K. Chembo, T. Hansson, S. Wabnitz, P. Del'Haye, X. Xue, A. M. Weiner, and R. Morandotti, "Micro-combs: A novel generation of optical sources," *Physics Reports*, vol. 729, pp. 1–81.

[29] P. Del'Haye, A. Schliesser, O. Arcizet, T. Wilken, R. Holzwarth, and T. J. Kippenberg, "Optical frequency comb generation from a monolithic microresonator," *Nature*, vol. 450, no. 7173, pp. 1214–1217.

[30] J. S. Levy, A. Gondarenko, M. A. Foster, A. C. Turner-Foster, A. L. Gaeta, and M. Lipson, "CMOS-compatible multiple-wavelength oscillator for on-chip optical interconnects," *Nature Photonics*, vol. 4, no. 1, pp. 37–40.

[31] J. Riemensberger, A. Lukashchuk, M. Karpov, W. Weng, E. Lucas, J. Liu, and T. J. Kippenberg, "Massively parallel coherent laser ranging using a soliton microcomb," *Nature*, vol. 581, no. 7807, pp. 164–170.

[32] P. J. Marchand, J. Riemensberger, J. C. Skehan, J.-J. Ho, M. H. P. Pfeiffer, J. Liu, C. Hauger, T. Lasser, and T. J. Kippenberg, "Soliton microcomb based spectral domain optical coherence tomography," *Nature Communications*, vol. 12, no. 1, p. 427.

[33] A. Dutt, C. Joshi, X. Ji, J. Cardenas, Y. Okawachi, K. Luke, A. L. Gaeta, and M. Lipson, "On-chip dual-comb source for spectroscopy," *Science Advances*, vol. 4, no. 3, p. e1701858, 2018.

[34] P. Trocha, M. Karpov, D. Ganin, M. H. P. Pfeiffer, A. Kordts, S. Wolf, J. Krockenberger, P. Marin-Palomo, C. Weimann, S. Randel, W. Freude, T. J. Kippenberg, and C. Koos, "Ultrafast optical ranging using microresonator soliton frequency combs," *Science*, vol. 359, no. 6378, pp. 887–891.

[35] M.-G. Suh, Q.-F. Yang, K. Y. Yang, X. Yi, and K. J. Vahala, "Microresonator soliton dual-comb spectroscopy," *Science*, vol. 354, no. 6312, pp. 600–603, 2016.

[36] H. Schnatz, B. Lipphardt, J. Helmcke, F. Riehle, and G. Zinner, "First phase-coherent frequency measurement of visible radiation," *Phys. Rev. Lett.*, vol. 76, pp. 18–21, 1996.

[37] S. A. Diddams, "The evolving optical frequency comb [invited]," *Journal of the Optical Society of America B*, vol. 27, no. 11, p. B51.

[38] S. A. Diddams, D. J. Jones, J. Ye, S. T. Cundiff, J. L. Hall, J. K. Ranka, R. S. Windeler, R. Holzwarth, T. Udem, and T. W. Hänsch, "Direct link between microwave and optical frequencies with a 300 THz femtosecond laser comb," *Physical Review Letters*, vol. 84, no. 22, pp. 5102–5105.

[39] S. A. Diddams, K. Vahala, and T. Udem, "Optical frequency combs: Coherently uniting the electromagnetic spectrum," *Science*, vol. 369, no. 6501, p. eaay3676.

[40] L. E. Hargrove, R. L. Fork, and M. A. Pollack, "Locking of he–ne laser modes induced by synchronous intracavity modulation," *Applied Physics Letters*, vol. 5, no. 1, pp. 4–5, 1964.

[41] H. W. Mocker and R. J. Collins, "Mode competition and self-locking effects in a q-switched ruby laser," *Applied Physics Letters*, vol. 7, no. 10, pp. 270–273, 1965.

[42] D. E. Spence, P. N. Kean, and W. Sibbett, "60-fsec pulse generation from a self-mode-locked ti: sapphire laser," *Optics letters*, vol. 16, no. 1, pp. 42–44, 1991.

[43] J. Reichert, R. Holzwarth, T. Udem, and T. W. Hänsch, "Measuring the frequency of light with mode-locked lasers," *Optics Communications*, vol. 172, no. 1-6, pp. 59–68, 1999.

[44] H. R. Telle, G. Steinmeyer, A. E. Dunlop, J. Stenger, D. H. Sutter, and U. Keller, "Carrier-envelope offset phase control: A novel concept for absolute optical frequency measurement and ultrashort pulse generation," *Applied Physics B*, vol. 69, no. 4, pp. 327–332, 1999.

[45] J. K. Ranka, R. S. Windeler, and A. J. Stentz, "Visible continuum generation in air–silica microstructure optical fibers with anomalous dispersion at 800 nm," *Optics Letters.*, vol. 25, no. 1, pp. 25–27, 2000.

[46] V. Torres-Company and A. M. Weiner, "Optical frequency comb technology for ultra-broadband radio-frequency photonics," *Laser & Photonics Reviews*, vol. 8, no. 3, pp. 368–393, 2014.

[47] R. Wu, V. Torres-Company, D. E. Leaird, and A. M. Weiner, "Supercontinuum-based 10-ghz flat-topped optical frequency comb generation," *Opt. Express*, vol. 21, no. 5, pp. 6045–6052, 2013.

[48] A. J. Metcalf, V. Torres-Company, D. E. Leaird, and A. M. Weiner, "High-power broadly tunable electrooptic frequency comb generator," *IEEE Journal of Selected Topics in Quantum Electronics*, vol. 19, no. 6, pp. 231–236, 2013.

[49] V. Torres-Company, J. Lancis, and P. Andrés, "Lossless equalization of frequency combs," *Optics Letters.*, vol. 33, no. 16, pp. 1822–1824, 2008.

[50] S. Xiao, L. Hollberg, N. R. Newbury, and S. A. Diddams, "Toward a low-jitter 10 ghz pulsed source with an optical frequency comb generator," *Opt. Express*, vol. 16, no. 12, pp. 8498–8508, 2008.

[51] L. Lundberg, M. Mazur, A. Fiilöp, V. Torres-Company, and M. Karlsson, "Phase correlation between lines of electro-optical frequency combs," in *2018 Conference on Lasers and Electro-Optics (CLEO)*, 2018, pp. 1–2.

[52] K. Beha, D. C. Cole, P. Del'Haye, A. Coillet, S. A. Diddams, and S. B. Papp, "Electronic synthesis of light," *Optica*, vol. 4, no. 4, pp. 406–411, 2017.

[53] D. R. Carlson, D. D. Hickstein, W. Zhang, A. J. Metcalf, F. Quinlan, S. A. Diddams, and S. B. Papp, "Ultrafast electro-optic light with subcycle control," *Science*, vol. 361, no. 6409, pp. 1358–1363, 2018.

[54] N. B. Hébert, V. Michaud-Belleau, C. Perrella, G.-W. Truong, J. D. Anstie, T. M. Stace, J. Genest, and A. N. Luiten, "Real-time dynamic atomic spectroscopy using electro-optic frequency combs," *Physical Review Applied*, vol. 6, no. 4, p. 044012, 2016.

[55] N. Wilson, N. B. Hébert, C. Perrella, P. Light, J. Genest, S. Pustelny, and A. Luiten, "Simultaneous observation of nonlinear magneto-optical rotation in the temporal and spectral domains with an electro-optic frequency comb," *Physical Review Applied*, vol. 10, no. 3, p. 034012, 2018.

[56] D. A. Long, A. J. Fleisher, D. F. Plusquellic, and J. T. Hodges, "Electromagnetically induced transparency in vacuum and buffer gas potassium cells probed via electro-optic frequency combs," *Optics Letters*, vol. 42, no. 21, pp. 4430–4433, 2017.

[57] D. R. Carlson, D. D. Hickstein, S. A. Diddams, and S. B. Papp, "High-speed ultra-broadband dual-comb spectroscopy using electro-optics," in *2018 Conference on Lasers and Electro-Optics (CLEO)*. IEEE, 2018, pp. 1–2.

[58] T. Nishikawa, A. Ishizawa, M. Yan, H. Gotoh, T. Hänsch, and N. Picqué, "Broadband dual-comb spectroscopy with cascaded-electro-optic-modulator-based frequency combs," in *CLEO: Science and Innovations*. Optical Society of America, 2015, pp. SW3G–2.

[59] P. Martin-Mateos, M. Ruiz-Llata, J. Posada-Roman, and P. Acedo, "Dual-comb architecture for fast spectroscopic measurements and spectral characterization," *IEEE Photonics Technology Letters*, vol. 27, no. 12, pp. 1309–1312, 2015.

[60] V. Durán, S. Tainta, and V. Torres-Company, "Ultrafast electrooptic dual-comb interferometry," *Opt. Express*, vol. 23, no. 23, pp. 30 557–30 569, 2015.

[61] F. Ferdous, D. E. Leaird, C.-B. Huang, and A. M. Weiner, "Dual-comb electric-field cross-correlation technique for optical arbitrary waveform characterization," *Optics Letters.*, vol. 34, no. 24, pp. 3875–3877, 2009.

[62] E. Deriushkina, I. R. Salgado, M. Mazur, V. Torres-Company, P. Andrekson, S. Gross, M. J. Withford, T. Hayashi, T. Nagashima, J. Schröder, and M. Karlsson, "Characterisation of a coupled-core fiber using dual-comb swept-wavelength interferometry," in *2021 European Conference on Optical Communication (ECOC)*, 2021, pp. 1–4.

[63] K. J. Vahala, "Optical microcavities," *Nature*, vol. 424, no. 6950, pp. 839–846, 2003.

[64] M. H. Dunn and M. Ebrahimzadeh, "Parametric generation of tunable light from continuous-wave to femtosecond pulses," *Science*, vol. 286, no. 5444, pp. 1513–1517, 1999.

[65] T. J. Kippenberg, S. M. Spillane, and K. J. Vahala, "Kerr-nonlinearity optical parametric oscillation in an ultrahigh-Q toroid microcavity," *Phys. Rev. Lett.*, vol. 93, p. 083904, 2004.

[66] A. A. Savchenkov, A. B. Matsko, D. Strekalov, M. Mohageg, V. S. Ilchenko, and L. Maleki, "Low threshold optical oscillations in a whispering gallery mode CaF_2 resonator," *Phys. Rev. Lett.*, vol. 93, p. 243905, 2004.

[67] P. Del'Haye, O. Arcizet, A. Schliesser, R. Holzwarth, and T. J. Kippenberg, "Full stabilization of a microresonator-based optical frequency comb," *Phys. Rev.Lett.*, vol. 101, p. 053903, 2008.

[68] J. Liu, E. Lucas, A. S. Raja, J. He, J. Riemensberger, R. N. Wang, M. Karpov, H. Guo, R. Bouchand, and T. J. Kippenberg, "Photonic microwave generation in the X- and K-band using integrated soliton microcombs," *Nature Photonics*, vol. 14, no. 8, pp. 486–491.

[69] J. Leuthold, C. Koos, and W. Freude, "Nonlinear silicon photonics," *Nature Photonics*, vol. 4, no. 8, pp. 535–544.

[70] T. Herr, V. Brasch, J. D. Jost, C. Y. Wang, N. M. Kondratiev, M. L. Gorodetsky, and T. J. Kippenberg, "Temporal solitons in optical microresonators," *Nature Photonics*, vol. 8, no. 2, pp. 145–152.

[71] T. J. Kippenberg, A. L. Gaeta, M. Lipson, and M. L. Gorodetsky, "Dissipative Kerr solitons in optical microresonators," *Science*, vol. 361, no. 6402, p. eaan8083, 2018.

[72] T. Herr, V. Brasch, J. D. Jost, C. Y. Wang, N. M. Kondratiev, M. L. Gorodetsky, and T. J. Kippenberg, "Temporal solitons in optical microresonators," *Nature Photonics*, vol. 8, no. 2, pp. 145–152, 2014.

[73] X. Xue, Y. Xuan, Y. Liu, P.-H. Wang, S. Chen, J. Wang, D. E. Leaird, M. Qi, and A. M. Weiner, "Mode-locked dark pulse Kerr combs in normal-dispersion microresonators," *Nature Photonics*, vol. 9, no. 9, pp. 594–600, 2015.

[74] V. Lobanov, G. Lihachev, T. Kippenberg, and M. Gorodetsky, "Frequency combs and platicons in optical microresonators with normal GVD," *Optics Express*, vol. 23, no. 6, pp. 7713–7721, 2015.

[75] P. Del'Haye, T. Herr, E. Gavartin, M. L. Gorodetsky, R. Holzwarth, and T. J. Kippenberg, "Octave spanning tunable frequency comb from a microresonator," *Phys. Rev. Lett.*, vol. 107, p. 063901, 2011.

[76] M.-G. Suh, X. Yi, Y.-H. Lai, S. Leifer, I. S. Grudinin, G. Vasisht, E. C. Martin, M. P. Fitzgerald, G. Doppmann, J. Wang *et al.*, "Searching for exoplanets using a microresonator astrocomb," *Nature photonics*, vol. 13, no. 1, pp. 25–30, 2019.

[77] C. Bao, M.-G. Suh, and K. Vahala, "Microresonator soliton dual-comb imaging," *Optica*, vol. 6, no. 9, pp. 1110–1116, 2019.

[78] M. Yu, Y. Okawachi, A. G. Griffith, M. Lipson, and A. L. Gaeta, "Microfluidic mid-infrared spectroscopy via microresonator-based dual-comb source," *Optics Letters.*, vol. 44, no. 17, pp. 4259–4262, 2019.

[79] Z. L. Newman, V. Maurice, T. Drake, J. R. Stone, T. C. Briles, D. T. Spencer, C. Fredrick, Q. Li, D. Westly, B. R. Ilic, B. Shen, M.-G. Suh, K. Y. Yang, C. Johnson, D. M. S. Johnson, L. Hollberg, K. J. Vahala, K. Srinivasan, S. A. Diddams, J. Kitching, S. B. Papp, and M. T. Hummon, "Architecture for the photonic integration of an optical atomic clock," *Optica*, vol. 6, no. 5, pp. 680–685, 2019.

[80] X. Ji, X. Yao, A. Klenner, Y. Gan, A. L. Gaeta, C. P. Hendon, and M. Lipson, "Chip-based frequency comb sources for optical coherence tomography," *Opt. Express*, vol. 27, no. 14, pp. 19 896–19 905, 2019.

[81] M. Yu, Y. Okawachi, A. G. Griffith, M. Lipson, and A. L. Gaeta, "Microresonator-based high-resolution gas spectroscopy," *Optics Letters.*, vol. 42, no. 21, pp. 4442–4445, 2017.

[82] M. Yu, Y. Okawachi, C. Joshi, X. Ji, M. Lipson, and A. L. Gaeta, "Gas-phase microresonator-based comb spectroscopy without an external pump laser," *ACS Photonics*, vol. 5, no. 7, pp. 2780–2785, 2018.

[83] Q.-F. Yang, X. Yi, K. Y. Yang, and K. Vahala, "Counter-propagating solitons in microresonators," *Nature Photonics*, vol. 11, no. 9, pp. 560–564.

[84] C. Joshi, A. Klenner, Y. Okawachi, M. Yu, K. Luke, X. Ji, M. Lipson, and A. L. Gaeta, "Counter-rotating cavity solitons in a silicon nitride microresonator," *Optics Letters*, vol. 43, no. 3, p. 547.

[85] M.-G. Suh and K. J. Vahala, "Soliton microcomb range measurement," *Science*, vol. 359, no. 6378, pp. 884–887.

[86] N. Singh, D. Vermulen, A. Ruocco, N. Li, E. Ippen, F. X. Kärtner, and M. R. Watts, "Supercontinuum generation in varying dispersion and birefringent silicon waveguide," *Optics Express*, vol. 27, no. 22, pp. 31 698–31 712, 2019.

[87] B. Kuyken, T. Ideguchi, S. Holzner, M. Yan, T. W. Hänsch, J. Van Campenhout, P. Verheyen, S. Coen, F. Leo, R. Baets, G. Roelkens, and N. Picqué, "An octave-spanning mid-infrared frequency comb generated in a silicon nanophotonic wire waveguide," *Nature Communications*, vol. 6, no. 1, pp. 1–6, 2015.

[88] R. Halir, Y. Okawachi, J. Levy, M. Foster, M. Lipson, and A. Gaeta, "Ultrabroadband supercontinuum generation in a CMOS-compatible platform," *Optics Letters*, vol. 37, no. 10, pp. 1685–1687, 2012.

[89] J. Liu, G. Huang, R. N. Wang, J. He, A. S. Raja, T. Liu, N. J. Engelsen, and T. J. Kippenberg, "High-yield, wafer-scale fabrication of ultralow-loss, dispersion-engineered silicon nitride photonic circuits," *Nature communications*, vol. 12, no. 1, pp. 1–9, 2021.

[90] A. R. Johnson, A. S. Mayer, A. Klenner, K. Luke, E. S. Lamb, M. R. Lamont, C. Joshi, Y. Okawachi, F. W. Wise, M. Lipson *et al.*, "Octave-spanning coherent supercontinuum generation in a silicon nitride waveguide," *Optics Letters*, vol. 40, no. 21, pp. 5117–5120, 2015.

[91] H. Hu, F. Da Ros, M. Pu, F. Ye, K. Ingerslev, E. Porto da Silva, M. Nooruzzaman, Y. Amma, Y. Sasaki, T. Mizuno *et al.*, "Single-source chip-based frequency comb enabling extreme parallel data transmission," *Nature Photonics*, vol. 12, no. 8, pp. 469–473, 2018.

[92] H. Jung, C. Xiong, K. Y. Fong, X. Zhang, and H. X. Tang, "Optical frequency comb generation from aluminum nitride microring resonator," *Optics Letters*, vol. 38, no. 15, pp. 2810–2813, 2013.

[93] A. L. Gaeta, M. Lipson, and T. J. Kippenberg, "Photonic-chip-based frequency combs," *Nature Photonics*, vol. 13, no. 3, pp. 158–169, 2019.

[94] J. M. Dudley and J. R. Taylor, *Supercontinuum generation in optical fibers.* Cambridge University Press, 2010.

[95] M. A. Foster, A. C. Turner, M. Lipson, and A. L. Gaeta, "Nonlinear optics in photonic nanowires," *Optics Express*, vol. 16, no. 2, pp. 1300–1320, 2008.

[96] G. P. Agrawal, *Nonlinear Fiber Optics*, 5th ed. Elsevier, 2012.

[97] J. M. Dudley and S. Coen, "Coherence properties of supercontinuum spectra generated in photonic crystal and tapered optical fibers," *Optics Letters.*, vol. 27, no. 13, pp. 1180–1182, 2002.

[98] C. Finot, B. Kibler, L. Provost, and S. Wabnitz, "Beneficial impact of wave-breaking for coherent continuum formation in normally dispersive nonlinear fibers," *J. Opt. Soc. Am. B*, vol. 25, no. 11, pp. 1938–1948, 2008.

[99] H. Guo, C. Herkommer, A. Billat, D. Grassani, C. Zhang, M. H. Pfeiffer, W. Weng, C.-S. Bres, and T. J. Kippenberg, "Mid-infrared frequency comb via coherent dispersive wave generation in silicon nitride nanophotonic waveguides," *Nature Photonics*, vol. 12, no. 6, pp. 330–335, 2018.

[100] A. M. Heidt, J. S. Feehan, J. H. Price, and T. Feurer, "Limits of coherent supercontinuum generation in normal dispersion fibers," *JOSA B*, vol. 34, no. 4, pp. 764–775, 2017.

[101] T. J. Kippenberg, R. Holzwarth, and S. A. Diddams, "Microresonator-based optical frequency combs," *Science*, vol. 332, no. 6029, pp. 555–559, 2011.

[102] T. Herr, V. Brasch, J. Jost, I. Mirgorodskiy, G. Lihachev, M. Gorodetsky, and T. Kippenberg, "Mode spectrum and temporal soliton formation in optical microresonators," *Physical Review Letters*, vol. 113, no. 12, p. 123901, 2014.

[103] T. Herr, K. Hartinger, J. Riemensberger, C. Wang, E. Gavartin, R. Holzwarth, M. Gorodetsky, and T. Kippenberg, "Universal formation dynamics and noise of Kerr-frequency combs in microresonators," *Nature Photonics*, vol. 6, no. 7, pp. 480–487, 2012.

[104] Y. Liu, Y. Xuan, X. Xue, P.-H. Wang, S. Chen, A. J. Metcalf, J. Wang, D. E. Leaird, M. Qi, and A. M. Weiner, "Investigation of mode coupling in normal-dispersion silicon nitride microresonators for kerr frequency comb generation," *Optica*, vol. 1, no. 3, pp. 137–144, 2014.

[105] P. Parra-Rivas, E. Knobloch, D. Gomila, and L. Gelens, "Dark solitons in the Lugiato-Lefever equation with normal dispersion," *Physical Review A*, vol. 93, no. 6, p. 063839, 2016.

[106] X. Xue, P. Wang, Y. Xuan, M. Qi, and A. M. Weiner, "Microresonator Kerr frequency combs with high conversion efficiency," *Laser & Photonics Reviews*, vol. 11, no. 1, p. 1600276.

[107] B. Y. Kim, Y. Okawachi, J. K. Jang, M. Yu, X. Ji, Y. Zhao, C. Joshi, M. Lipson, and A. L. Gaeta, "Turn-key, high-efficiency kerr comb source," *Optics Letters.*, vol. 44, no. 18, pp. 4475–4478, 2019.

[108] Ó. B. Helgason, F. R. Arteaga-Sierra, Z. Ye, K. Twayana, P. A. Andrekson, M. Karlsson, J. Schröder, and V. Torres-Company, "Dissipative solitons in photonic molecules," *Nature Photonics*, vol. 15, no. 4, pp. 305–310, 2021.

[109] L. A. Lugiato and R. Lefever, "Spatial dissipative structures in passive optical systems," *Physical Review Letters*, vol. 58, no. 21, p. 2209, 1987.

[110] S. Coen and M. Haelterman, "Modulational instability induced by cavity boundary conditions in a normally dispersive optical fiber," *Physical review letters*, vol. 79, no. 21, p. 4139, 1997.

[111] Ó. B. Helgason, M. Girardi, Z. Ye, F. Lei, J. Schröder, and V. T. Company, "Power-efficient soliton microcombs," *arXiv preprint arXiv:2202.09410*, 2022.

[112] N. Picqué and T. W. Hänsch, "Frequency comb spectroscopy," *Nature Photonics*, vol. 13, no. 3, pp. 146–157.

[113] S. A. Diddams, L. Hollberg, and V. Mbele, "Molecular fingerprinting with the resolved modes of a femtosecond laser frequency comb," *Nature*, vol. 445, no. 7128, pp. 627–630.

[114] P. Maslowski, K. F. Lee, A. C. Johansson, A. Khodabakhsh, G. Kowzan, L. Rutkowski, A. A. Mills, C. Mohr, J. Jiang, M. E. Fermann, and A. Foltynowicz, "Surpassing the path-limited resolution of Fourier-transform spectrometry with frequency combs," *Phys. Rev. A*, vol. 93, p. 021802, 2016.

[115] L. Rutkowski, P. Masłowski, A. C. Johansson, A. Khodabakhsh, and A. Foltynowicz, "Optical frequency comb fourier transform spectroscopy with sub-nominal resolution and precision beyond the Voigt profile," *Journal of Quantitative Spectroscopy and Radiative Transfer*, vol. 204, pp. 63–73, 2018.

[116] A. Głuszek, F. Senna Vieira, A. Hudzikowski, A. Wąż, J. Sotor, A. Foltynowicz, and G. Soboń, "Compact mode-locked er-doped fiber laser for broadband cavity-enhanced spectroscopy," *Applied Physics B*, vol. 126, no. 8, pp. 1–6, 2020.

[117] A. C. Johansson, L. Rutkowski, A. Khodabakhsh, and A. Foltynowicz, "Signal line shapes of fourier-transform cavity-enhanced frequency modulation spectroscopy with optical frequency combs," *J. Opt. Soc. Am. B*, vol. 34, no. 2, pp. 358–365, 2017.

[118] I. Coddington, N. Newbury, and W. Swann, "Dual-comb spectroscopy," *Optica*, vol. 3, no. 4, p. 414.

[119] Z. Chen, M. Yan, T. W. Hänsch, and N. Picqué, "A phase-stable dual-comb interferometer," *Nature Communications*, vol. 9, no. 1, pp. 1–7, 2018.

[120] Z. Chen, T. W. Hänsch, and N. Picqué, "Mid-infrared feed-forward dual-comb spectroscopy," *Proceedings of the National Academy of Sciences*, vol. 116, no. 9, pp. 3454–3459, 2019.

[121] F. Keilmann, C. Gohle, and R. Holzwarth, "Time-domain mid-infrared frequency-comb spectrometer," *Optics Letters.*, vol. 29, no. 13, pp. 1542–1544, 2004.

[122] C. Erny, K. Moutzouris, J. Biegert, D. Kühlke, F. Adler, A. Leitenstorfer, and U. Keller, "Mid-infrared difference-frequency generation of ultrashort pulses tunable between 3.2 and 4.8 μm from a compact fiber source," *Optics Letters.*, vol. 32, no. 9, pp. 1138–1140, 2007.

[123] S. Schiller, "Spectrometry with frequency combs," *Optics Letters.*, vol. 27, no. 9, pp. 766–768, 2002.

[124] A. Weiner, *Ultrafast optics*. John Wiley & Sons, 2011, vol. 72.

[125] G. Millot, S. Pitois, M. Yan, T. Hovhannisyan, A. Bendahmane, T. W. Hänsch, and N. Picqué, "Frequency-agile dual-comb spectroscopy," *Nature Photonics*, vol. 10, no. 1, pp. 27–30, 2016.

[126] M. Karpov, H. Guo, A. Kordts, V. Brasch, M. H. P. Pfeiffer, M. Zervas, M. Geiselmann, and T. J. Kippenberg, "Raman self-frequency shift of dissipative kerr solitons in an optical microresonator," *Phys. Rev. Lett.*, vol. 116, p. 103902, 2016.

[127] E. Lucas, G. Lihachev, R. Bouchand, N. G. Pavlov, A. S. Raja, M. Karpov, M. L. Gorodetsky, and T. J. Kippenberg, "Spatial multiplexing of soliton microcombs," *Nature Photonics*, vol. 12, no. 11, pp. 699–705, 2018.

[128] A. S. Raja, J. Liu, N. Volet, R. N. Wang, J. He, E. Lucas, R. Bouchand, P. Morton, J. Bowers, and T. J. Kippenberg, "Packaged photonic chip-based soliton microcomb using an ultralow-noise laser," *arXiv preprint arXiv:1906.03194*, 2019.

[129] Q.-F. Yang, Q.-X. Ji, L. Wu, B. Shen, H. Wang, C. Bao, Z. Yuan, and K. Vahala, "Dispersive-wave induced noise limits in miniature soliton microwave sources," *Nature Communications*, vol. 12, no. 1, pp. 1–10, 2021.

[130] X. Yi, Q.-F. Yang, K. Y. Yang, and K. Vahala, "Imaging soliton dynamics in optical microcavities," *Nature Communications*, vol. 9, no. 1, p. 3565.

Included papers A-C

Paper A

Israel Rebolledo-Salgado, Zhichao Ye, Simon Christensen, Fuchuan Lei, Krishna Twayana, Jochen Schröder, Martin Zelan, and Victor Torres-Company, "Coherent supercontinuum generation in all-normal dispersion Si_3N4 waveguides", *Optics Express*, 30, 8641-8651, 2022.

Paper B

Israel Rebolledo-Salgado1, Óskar B. Helgason, Zhichao Ye, Jochen Schröder, Martin Zelan, and Victor Torres-Company, "Photonic molecule microcombs at 50 GHz repetition rate", *Conference on Lasers and Electro-Optics*, San Jose, USA, paper SW4O.8, 2022

Paper C

Krishna Twayana, Israel Rebolledo-Salgado, Ekaterina Deriushkina, Jochen Schröder, Magnus Karlsson and Victor Torres-Company, "Frequency-comb-based spectral interferometry for characterization of photonic devices", *Micromachines*, 13, no 4, p. 614, 2022.